

$$= \frac{1}{(1-s^2)^{1/2}} + \frac{2s^2}{(1-s^2)^{3/2}} - \frac{\log[2(1-s^2)]}{(1-s^2)^{3/2}} \quad (7)$$

Substitution of Eqs. (6) and (7) into Eq. (5) results in

$$\frac{\Gamma}{\Gamma_\infty} = 1 - \frac{2}{A} - \frac{4}{\pi^2} \frac{\log A}{A^2} \frac{3-2s^2}{1-s^2} + \frac{4}{\pi^2} \frac{1}{A^2} \left\{ \pi^2 + \frac{5}{2} - \frac{3-2s^2}{1-s^2} \right. \\ \left. \log \frac{\pi}{(1-s^2)^{1/2}} - \log(1-s^2) + \frac{2s^2}{1-s^2} - \frac{\log[2(1-s^2)]}{1-s^2} \right\} \\ + o(A^{-2}) \quad (8)$$

which differs from Eq. (3.10) of Ref. 1 in the coefficient of A^{-2} . Finally, the lift-curve slope is found using Eqs. (1, 4, and 8) and Eqs. (864.31) and (864.32) of Ref. 5 as

$$\frac{dC_L}{d\alpha} = 2\pi \left[1 - \frac{2}{A} - \frac{16}{\pi^2} \frac{\log A}{A^2} + \frac{4}{\pi^2} \frac{1}{A^2} \left(\frac{9}{2} + \pi^2 - 4 \log \pi \right) \right] + o(A^{-2}) \quad (9)$$

Equation (9) differs from Eq. (3.11) of Ref. 1 in the presence of $9/2$ in place of $7/2$. If the series is recast as a fraction the 7 in Eq. (3.13) of Ref. 1, Eq. (10.27) of Ref. 2, and Eq. (12) of Ref. 6 should be replaced by 9 .

References

- 1 Van Dyke, M., "Lifting-Line Theory as a Singular Perturbation Problem," *Archiwum Mechaniki Stosowanej*, Vol. 16, No. 3, 1964, pp. 601-614; also Rept. 165, Aug. 1963, Dept. of Aeronautics and Astronautics, Stanford Univ.; also *Fluid Dynamics Transactions*, Vol. 2, Pergamon Press, Oxford, 1965, pp. 369-382; also *Journal of Applied Mathematics and Mechanics*, Vol. 28, No. 1, Oct. 1964, pp. 90-102.
- 2 Van Dyke, M., *Perturbation Methods in Fluid Mechanics*, Academic Press, New York, 1964, Secs. 9.2-9.5.
- 3 Van Dyke, M., "Second-Order Subsonic Airfoil Theory including Edge Effects," Rept. 1274, 1956, NACA.
- 4 Heaslet, M. A. and Lomax, H., "Supersonic and Transonic Small-Perturbation Theory," *General Theory of High-Speed Aerodynamics*, edited by W. R. Sears, Princeton University Press, Princeton, N. J., 1954, Sec. 14.1.
- 5 Dwight, H. B., *Tables of Integrals and Other Mathematical Data*, 4th ed., MacMillan, New York, 1961.
- 6 Germain, P., "Recent Evolution in Problems and Methods in Aerodynamics," *Journal of the Royal Aeronautical Society*, Vol. 71, No. 682, Oct. 1967, pp. 673-691.

Prandtl Eddy Viscosity Model for Coaxial Jets

HERMANN VIETS*

Aerospace Research Laboratories/LE,
Wright-Patterson Air Force Base, Ohio

A RECENT paper by Harsha¹ presents a rather complete comparison with experimental data of freejet calculations employing eddy viscosity models. One of the conclusions is that of all the theoretical models depending solely on the local mean flow properties, the Prandtl² eddy viscosity model produces the best agreement in the far field of an incompressible axisymmetric jet into calm surroundings. However, with the addition of a coflowing stream, the success of the Prandtl model deteriorates rapidly. In this case the recommended model is due to Ferri, Libby, and Zakkay.³ For incompressible flow, Ferri's model reduces to Prandtl's model with a larger constant. Thus its

Received April 19, 1972; revision received June 30, 1972. Prepared under Contract F33615-71-C-1463 with Technology Inc., Dayton, Ohio. Thanks are due to B. P. Quinn and P. M. Bevilacqua for their helpful comments and V. Grycz for typing the manuscript.

Index categories: Jets, Wakes, and Viscid-Inviscid Flow Interactions.

* Visiting Research Associate. Member AIAA.

predictions are not really improved but rather shifted. It is the purpose of this Note to demonstrate that the inclusion of a simple nondimensional term in the Prandtl model can greatly increase the success of the predictions in the far field of the incompressible coaxial jet.

Prandtl's model of the eddy viscosity ϵ , is

$$\epsilon = kb(u_{\max} - u_{\min}) \quad (1)$$

where k is an empirical constant, b is proportional to the width of the mixing region and u_{\max} and u_{\min} are the maximum and minimum values of streamwise velocity at a given streamwise position.

The ability of the Prandtl model to predict the axis velocity decay of coaxial jets is shown in Fig. 1. The centerline velocity u , and the coflowing stream velocity u_e , are equivalent to u_{\max} and u_{\min} , respectively. The initial velocity of the jet is U , while the velocity ratio is $m \equiv u_e/U$. The const in the Prandtl model is chosen as $k = 0.007$ in the region $u > 0.99U$ and $k = 0.011$ downstream of that region. The half width, b , is defined as the distance between positions on the velocity profile where the velocity is equal to half the centerline velocity.

A reasonable curve fit of the available data¹ is indicated by the heavy line decaying at x^{-1} (i.e., 45° slope). It may be seen that the agreement of the Prandtl model deteriorates as the velocity ratio m increases.

The Ferri model was formulated to account for mixing in variable density flows. When simplified to the incompressible case, it reduces to the Prandtl model with a higher const, $k = 0.025$. The results of this model are also shown in Fig. 1. The intersection point of the Prandtl model with the empirical curve has moved downstream somewhat, resulting in better agreement near that point. However, the far field decay slope still is not matched very well.

The original development of the Prandtl model assumed that the dimensions of the lumps of fluid which are transported across the jet are of the same order of magnitude as the width of the mean shear layer. That this assumption is affected by the addition of a coflowing stream may be seen in the limit where the coflowing stream velocity is equal to the jet velocity and the width of the mean shear layer is zero. The flow is, however, still turbulent and the lumps of fluid transported by the turbulence are of finite size. Thus as the coflowing stream velocity increases, the size of the fluid lumps can be substantially larger than the width of the shear layer. Increasing the dimensions of the fluid lumps is equivalent to increasing the magnitude of the effective viscosity. To incorporate this effect into the Prandtl model, the eddy viscosity is increased by a term inversely proportional to the local velocity difference between the jet and freestream $(U - u_e)/(u - u_e)$.

The denominator of the preceding term is equivalent to the $(u_{\max} - u_{\min})$ term in the Prandtl model, so if the Prandtl model were simply multiplied by the coflowing stream modification, the local velocity difference terms, $(u - u_e)$, would cancel out and the resulting eddy viscosity would be proportional to the half width alone. To avoid this, the modification factor is raised to a power characteristic of the flow situation, the ratio of the coflowing stream velocity to the jet velocity, m .

The use of the velocity ratio as the exponent in the modification term may be viewed as follows. The shortcoming of the Prandtl

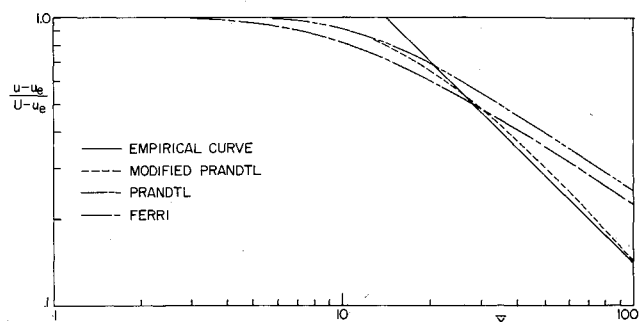


Fig. 1 Axial velocity decay; velocity ratio = 0.67.

model in the coflowing stream case is its inability to match the exponential decay rate of the jet. The experimental decay rate exponent is dependent upon the velocity ratio, while the Prandtl model exponent is equal to unity. The present modification improves the model by making the exponential decay rate dependent upon the initial velocity ratio. The resulting modified Prandtl eddy viscosity model is

$$\varepsilon = kb(u - u_e)[(U - u_e)/(u - u_e)]^m \quad (2)$$

Thus the Prandtl model is simply multiplied by the inverse of the quantity usually plotted as the ordinate of the velocity decay plots, raised to the power of the velocity ratio. In the case of the absence of a coflowing stream, the modified Prandtl model reduces identically to the classical Prandtl model.

The ability of the modified Prandtl model to predict the far field decay of coaxial jet is shown in Fig. 1. The new model successfully predicts the centerline velocity decay from approximately $\bar{x} = 20$ downstream.

References

- ¹ Harsha, P. T., "Free Turbulent Mixing: A Critical Evaluation of Theory and Experiment," TR 71-36, Feb. 1971, Arnold Engineering Development Center, Arnold Air Force Station, Tenn.
- ² Prandtl, L., "Bemerkungen zur Theorie der freien Turbulenz," *Zeitschrift für Angewandte Mathematik und Mechanik*, Vol. 22, Oct. 1942, pp. 241-243.
- ³ Ferri, A., Libby, P. A., and Zakkay, V., "Theoretical and Experimental Investigation of Supersonic Combustion," PIBAL 713, Sept. 1962, Polytechnic Institute of Brooklyn, Farmingdale, N. Y.

Base Pressure Distribution of a Cone at Hypersonic Speeds

GEORGE S. PICK*

Naval Ship Research and Development Center,
Bethesda, Md.

Nomenclature

M	= freestream Mach number
p_B	= base pressure
p_∞	= freestream static pressure
r	= radial distance from the centerline
R	= maximum base radius
Re	= unit Reynolds number
α	= angle of attack

Introduction

LITTLE or no data are available on base pressure distributions at high angles of attack in the hypersonic speed range. This is mainly due to the complex nature of the flowfield surrounding a three-dimensional body and the difficulties involved with measurements in the near wake. Therefore, the basic objective of the current work was to obtain reliable, interference-free base pressure distribution data on a 10° half-angle sharp, flat-based cone at high angles of attack (0 to 80°) and at hypersonic speeds ($M = 5.30, 6.34$, and 9.94) with varying Reynolds number ($Re = 3.0, 6.4, 11.2 \times 10^5/\text{ft}$). To this end, freeflying instrumented models were developed and tested in a freejet hypersonic facility. They were designed to be injected into the flowfield at predeter-

Presented as Paper 72-316 at the AIAA 7th Thermophysics Conference, San Antonio, Texas, April 10-12, 1972; submitted April 21, 1972; revision received June 19, 1972.

Index categories: Jets, Wakes and Viscid-Inviscid Flow Interactions, Supersonic and Hypersonic flow.

* Senior Aerospace Engineer, Aviation and Surface Effects Department, Aerodynamics Division. Member AIAA.

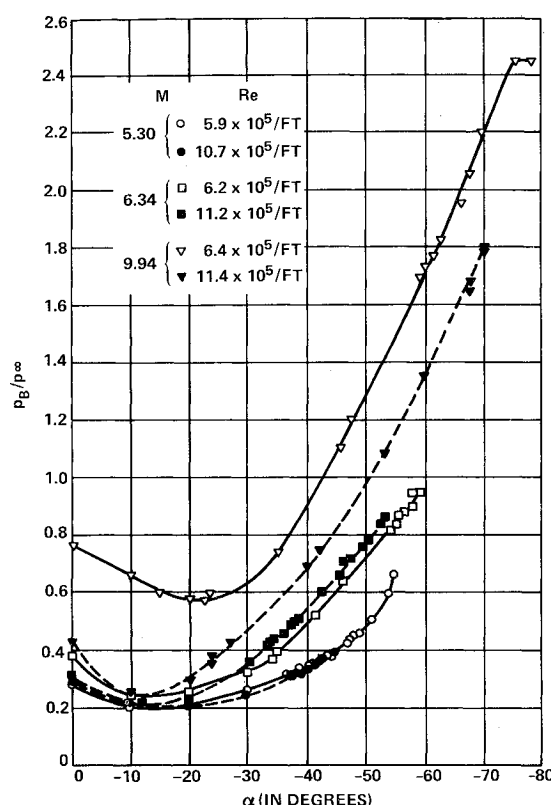


Fig. 1 Centerline base pressure ratio as function of angle of attack M and Re .

mined angles of attack and roll and to be released with adequate vertical velocity to fly through the test section. The decision to use free-flying models was based on reported data on sting interference as well as Pick's more recent investigation.¹

Description of Experimental Techniques

All experiments were conducted in the NAVSHIPRANDCEN variable Reynolds number hypersonic tunnel with a 13.5-in. open-jet test section. The 10° half-angle cone models used in the test program were 6 in. long and the outer shells were machined from stainless steel. A conical brass weight and threaded slugs, attached to the forward part of the model interior, provided for center-of-gravity adjustment. Four differential pressure transducer telemeters were the principal instrumentation and were located in the aft portion of the conical shell. Detailed performance characteristics and construction of these units are described by Harrison.² A mercury battery pack provided the power supply to the transducers. The transducer measuring ports were connected to the base plate at $r/R = 0, 0.24, 0.47$, and 0.71 .

Signals from the telemetry units were intercepted by a folded dipole antenna that was completely outside the hypersonic stream and connected to a signal conditioning and processing network. The incoming data were recorded on a multichannel oscillograph. Two high-speed motion picture cameras recorded the motions of the model. Computer programs converted the information from the oscillograph records and high-speed motion pictures to base pressure ratios p_B/p_∞ , angles of attack as functions of time. Optical lens distortions and human errors in data reduction were internally compensated for in the computations.

Prior to its injection into the hypersonic jet stream, the model was guided by a specially constructed drop mechanism that held it at a predetermined pitch angle. As the model was completely submerged into the inviscid core of the jet flow, the restraining arms opened and released the model. Within 10 msec from the initial release, the drop mechanism moved out of the flowfield to ensure disturbance-free conditions. The average available flight time, during which interference-free data were obtained,